# Switchable T-Slot for Dual-Circularly-Polarized Slot-Array Antennas in Ka-Band

Miguel Ferrando-Rocher, *Member, IEEE,* Jose I. Herranz-Herruzo, *Member, IEEE,*
Alejandro Valero-Nogueira, *Senior Member, IEEE,* Bernardo Bernardo-Clemente

***Abstract*—This paper presents two slotted array antennas working in the Ka-band with switchable circular polarization capability. The first prototype is a series-fed slotted-waveguide linear array composed of ten T-shaped slots. The second antenna is a two-dimensional array with 2×2 T-shaped slots fed by a corporate distribution network. In both cases, a reflection coefficient below −10 dB has been experimentally observed within the targeted frequency band between 29.5 and 30.5 GHz. Good polarization purity is achieved for both polarization senses and in both prototypes. The fundamental contribution of the paper is to propose a simple mechanism to switch the circular polarization sense in a low-cost, low-profile and high-efficient antenna. The design and experimental results confirm that the solution is suitable for both one- and two-dimensional arrays in the millimeter-wave band.**

***Index Terms*—Array, Dual-Circular Polarization, Gap Waveguide, Ka-Band, SATCOM.**

## I. Introduction

NEW Ka-band high throughput satellite (HTS) systems make use of multibeam solutions to cover continental regions. For example, around 80 beams are planned for the European continent alone [1] with orthogonal circular polarization and frequency diversity. In mobile end-user systems, such as trains or airplanes, wideband devices capable of switching polarization sense are strongly required [2], [3].

In this context, today exists a significant demand for higher-gain, lower-profile, simpler, cheaper solutions and easy to manufacture up to millimeter-wave frequencies. Due to such need, it is not difficult to find recent contributions addressing the problem from different perspectives. In general, two methodologies are commonly followed. On the one hand, reconfigurable radiators as in [4], [5], [6] and, on the other hand, complex reconfigurable feeding networks as in [7], [8], [9]. In general terms, these patch-based contributions suffer from low antenna efficiency.

Some recent contributions comply with various of the above mentioned requirements. For example, [10], [11] propose all-metal structures to play the role of polarization converters, with an evident benefit in terms of antenna efficiency and reliability. However, these kind of solutions lead to bulky structures, being impractical for the lowest band of the millimeter-wave spectrum. Very recently, in [12] an all-metal CP radiating element, able to convert the LP field radiated by a rectangular slot into a CP field in a very low-profile structure is presented. However, while all these designs achieve circular polarization in high efficiency antennas, they do not provide switching capability. Finally, it should be noted that certainly there exist some interesting approaches that achieve circular polarization switching either mechanically [13], [14] or electronically [15], [16]. Yet, architectures providing circular polarization switching is still a major challenge in Ka-band.

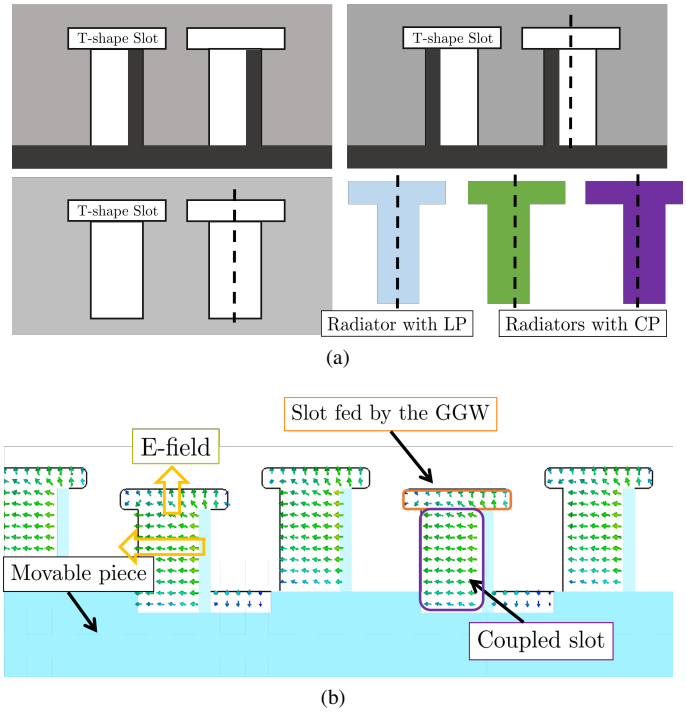


Fig. 1: (a) Schematic drawing of the structure. Metal of the fixed part is colored in grey. Dark grey represents the sliding aluminum comb. The standalone T-slot provides linear polarization. By decentering the T-slot with the movable piece, RH- or LH- circular polarization is achieved. (b) E-field distribution.

Here, the concept described in [12] is extended to mechanically switch between both rotation senses of circular polarization in a very simple way. While [12] is the starting point of the approach, two key issues are provided in this contribution: firstly, the experimental validation of a circular polarization switching mechanism in a linear array. Secondly, and more importantly, the idea is described and proved to be extensible to bi-dimensional arrays. This fact is not minor since the ultimate goal of this mechanism would be to use it in high-efficiency bi-dimensional flat panel antennas (FPA) for satellite communication (SATCOM) applications, which normally require a switchable circular polarization. Such

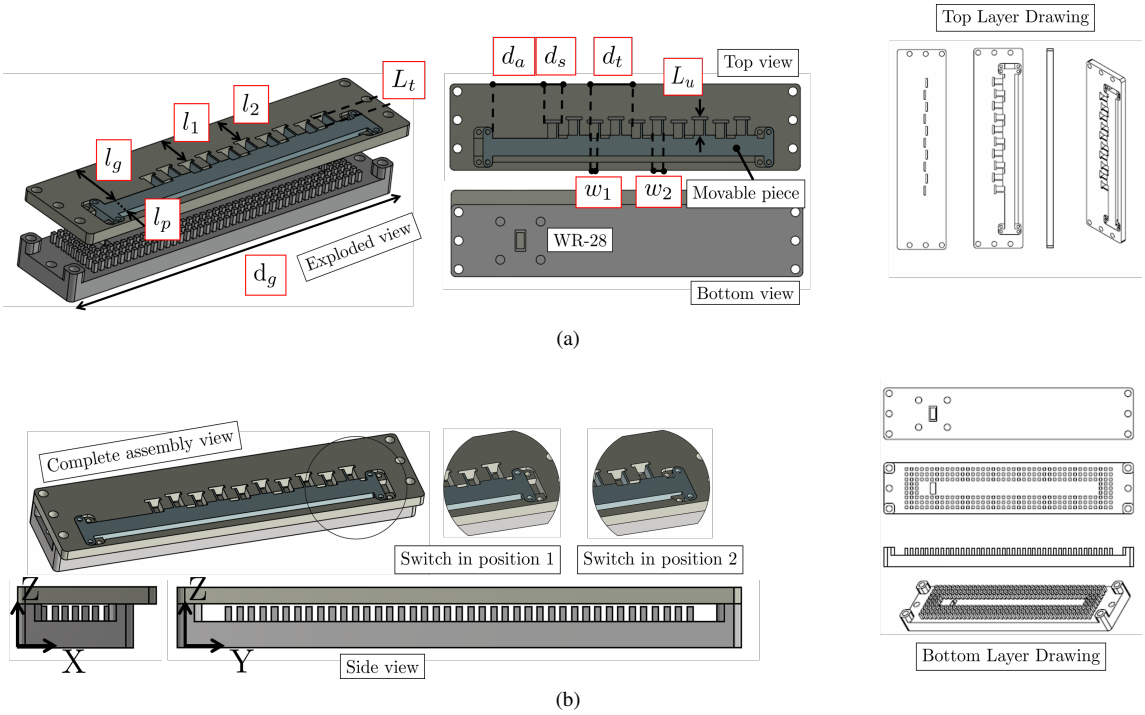


Fig. 2: 3D sketch of the 1×10 array antenna. (a) Left figure shows both lower and upper pieces of the antenna in an exploded view. The upper piece is composed of a fixed and a movable part, with different color for an easier identification. Top and bottom view are included in the right figure. (b) Complete assembled antenna (top and side views) with two zoomed figures showing the switching positions. Both figures include also top and bottom schematic drawings of the antenna.

switching need not be instantaneous and can be mechanical, such as the solution described here.

The paper is structured as follows. Section II describes each antenna in detail in two separate subsections: one for a series-fed antenna and the other for a corporate-fed one. The experimental validation of the proposed concept is reported for both manufactured prototypes in Section III. Finally, Section IV draws the main conclusions.

## II. Switchable T-Shape Slot

This section will describe two slotted waveguide antennas, a 1×10 array and a 2×2 array. In both cases the same switching structure is used, which is schematically depicted in Fig.1.

### A. 1-D Array design

Basically, the 1-D array consists of 10 series-fed T-shaped slots. A very preliminary description of this antenna was firstly used in [17] but without any experimental validation. There, some simulated results can be consulted. A complete description of the antenna is given here, providing the dimensions of all relevant parameters. In addition, the antenna is now fabricated and experimentally measured.

Fig. 2a shows the radiating layer of the antenna. This layer is composed of two pieces: one fixed and the other movable. The rear side of the fixed piece is a conventional shunt slot array, which feeds the T-shaped slots drilled in the upper face. The movable piece then plays a key role. Depending on the position to which it is shifted, the wider coupled arm of the T-shape will be off-center, on the left or on the right side, with respect to the feeding rectangular slot. In addition, the lid is fed through a groove gap waveguide (see Fig. 2b), which confines the field within the waveguide even though it has no contact with the top cover, as demonstrated in [18]-[19]. Observe how, in the side view of the antenna (Fig. 2b), there exists an air gap ($a_g$=556$\mu$m) between the nails and the lid. The nails of the bed are 3 mm in height, their side is 1.25 mm wide and they are periodically spaced by 2.4 mm. The entire contour of the GGW is surrounded by 3 rows of these nails. The excitation of the waveguide is done through a port at the bottom of the antenna that corresponds to a standard WR−28 flange. The distance from the center of this port to the short of the waveguide is approximately $\lambda_g/2$. The cover with the two metallic pieces, the fixed and the movable ones, is placed on top of this GGW.

A zoomed detail of the mechanism is shown in the right side of Fig. 2b. It can be seen how the comb can mechanically switch from one position to the other. The thickness of the fixed piece is 3.5 mm. One side of the fixed piece is emptied to leave space to accommodate the movable piece. Then, the thickness of the moving piece is 1.75 mm and it has a width of 5.9 mm. This metal tongue holds the comb spikes, which are spaced 7 mm apart. Finally, all relevant geometrical values of this antenna are shown in Table I.

### B. 2-D Array design

Now, it is presented how to adapt the mechanism for not only one-dimensional arrays but also for two-dimensional

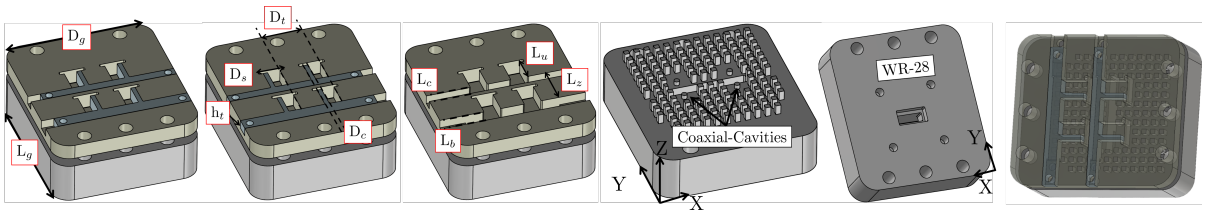


(a)

Fig. 3: 3D sketch of the 2×2 array antenna. From left to right, the first figure shows the complete assembled antenna. There, the movable piece is located in position 1. Second figure also shows the assembled antenna but with movable piece in position 2. In the third figure the movable piece has been removed for a better identification and visualization of the lid. The two rightmost figures correspond to the coaxial-fed cavity-backed slots and the input port through WR-28 standard flange, respectively.

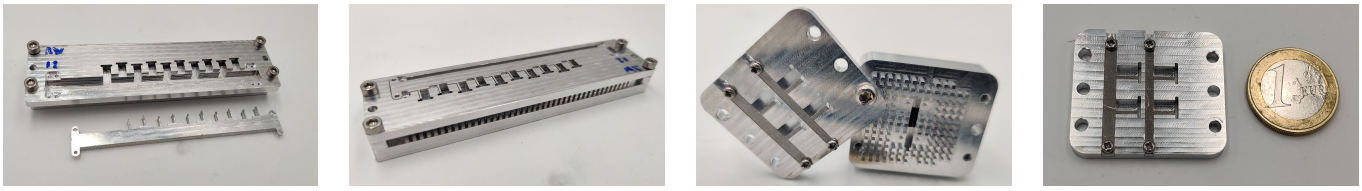

(a) (b) (c) (d)

Fig. 4: Manufactured prototypes: (a) complete 1×10 manufactured antenna. The movable piece of the lid has been placed aside for better visualization of the fixed lid; (b) fully assembled 1×10 slot array; (c) complete 2×2 manufactured antenna with the cover slipped out and (d) top view of the 2×2 antenna.

TABLE I: Dimensions of the 1×10 slot array.

| Parameter | Value (mm) | Parameter | Value (mm) |
|---|---|---|---|
| $d_g$ | 97.3 | $l_g$ | 18.1 |
| $w_1$ | 3.0 | $l_1$ | 12.0 |
| $w_2$ | 3.6 | $l_2$ | 10.9 |
| $d_s$ | 5.5 | $l_p$ | 5.9 |
| $d_t$ | 14.0 | $L_t$ | 5.1 |
| $d_a$ | 21.8 | $L_u$ | 6.1 |

TABLE II: Dimensions of the 2×2 slot array.

| Parameter | Value (mm) | Parameter | Value (mm) |
|---|---|---|---|
| $D_t$ | 9.0 | $L_c$ | 2.0 |
| $D_c$ | 1.0 | $L_u$ | 7.1 |
| $D_s$ | 5.7 | $L_z$ | 9.0 |
| $D_g$ | 26.0 | $L_g$ | 26.0 |
| $h_t$ | 2.0 | $L_b$ | 2.9 |

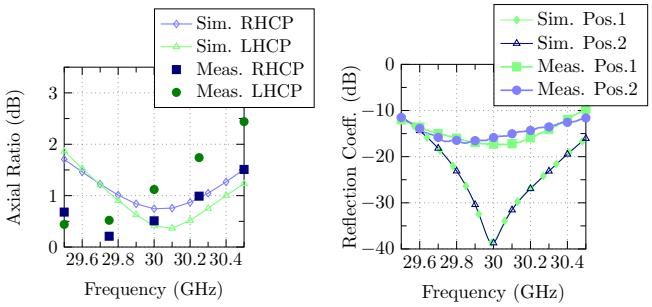


(a) (b)

Fig. 5: Results of the 1×10 series-fed array for each piece position: (a) Measured and simulated axial ratio and (b) measured and simulated reflection coefficient.

ones. Note that the lid described for the series-fed array is

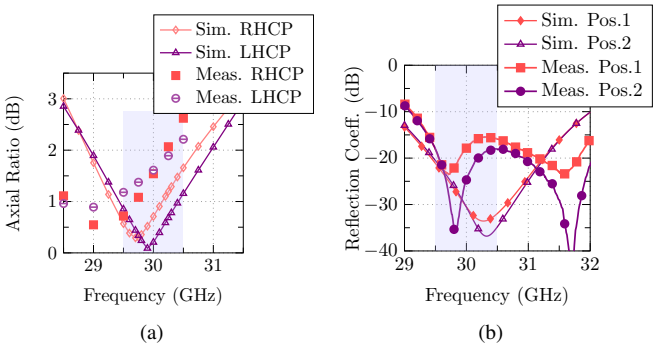


(a) (b)

Fig. 6: Results of the 2×2 corporate-fed array antenna for each piece position: (a) Measured and simulated axial ratio and (b) measured and simulated reflection coefficient.

fully valid to transform the linear polarization into a circular one and, at the same time, to switch between both circular polarization senses, RHCP and LHCP. Usefully, just a small modification is enough to adapt the idea for a two-dimensional array. Fig. 3 shows from left to right the complete cover, the fixed and the movable part, respectively. Obviously, being a two-dimensional array in this case, two combs are needed. A metal arm connects both combs making the moving part U-shaped. All relevant dimensions of this new part are indicated again, and are detailed in the Table II.

The fourth sketch of Fig. 3 shows the cavities that are backing the slots. It consists of 4 coaxial cavities excited by a central groove which in turn is fed by a slot coupled from the input port. This type of coaxial cavities in gap waveguide technology have been used and fully described in the past in [20], [21].

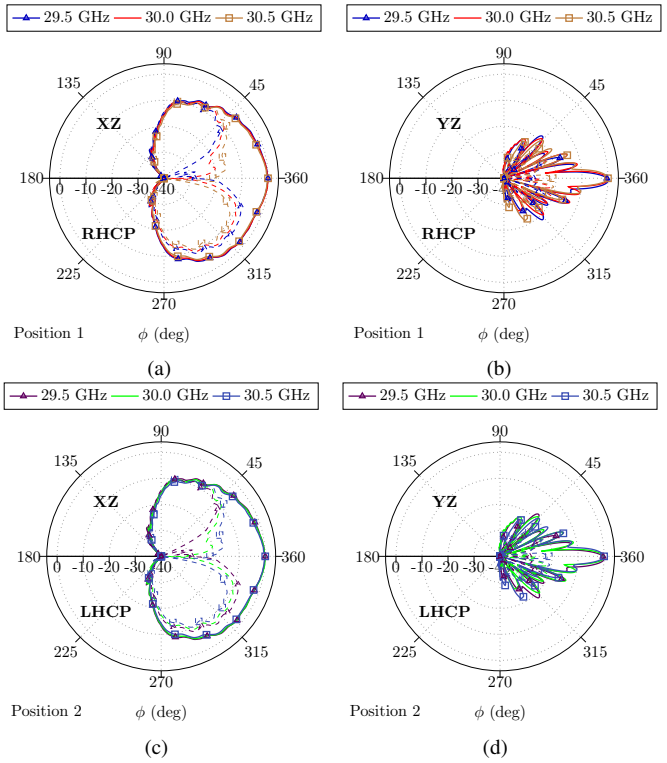


Fig. 7: Measured radiation patterns of the 1×10 array in a polar representation. Upper plots correspond to position 1 (RHCP), lower plots to position 2 (LHCP): (a) XZ plane and (b) YZ plane, (c) XZ plane and (d) YZ plane.

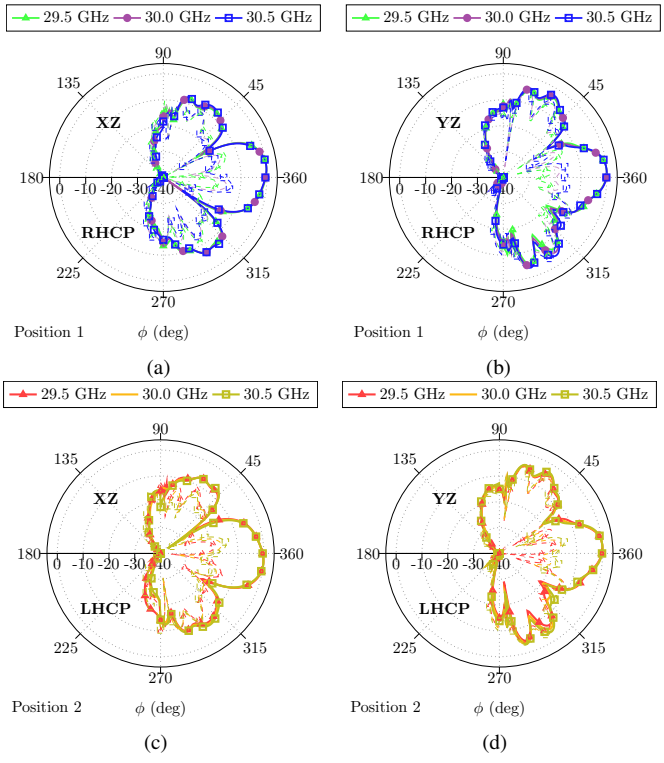


Fig. 8: Measured radiation patterns of the 2×2 array in a polar representation. Upper plots correspond to position 1 (RHCP), lower plots to position 2 (LHCP): (a) XZ plane and (b) YZ plane, (c) XZ plane and (d) YZ plane.

## III. Experimental validation

Both fabricated prototypes are shown in several pictures in Fig. 4. Likewise, both prototypes have been fabricated in-house in the Antennas and Propagation Laboratory facilities with a milling machine. The unique material used in both cases is AL7079 aluminum. Being the two prototypes fully metallic, high radiation efficiencies, above 80% in both cases, have been measured. Table III shows the measured gain for both antennas and for both switching positions at five frequency points within the band. Anyhow, the main objective of this study is to test the feasibility of circular polarization switching, which is verified in Figs. 5 to 8. Fig. 5 shows the measured and simulated axial ratio (AR) in the band of interest. Good polarization purity is obtained for both positions, with a maximum measured AR less than 2.5 dB in either case. It can be observed how the purest circular polarization occurs around 29.75 GHz, when a minimum AR centered at 30 GHz was expected. This displacement of the AR is mainly due to the effect of the screws used to fix the bottom and top pieces. These screws would presumably have a minor effect on a larger array. Fig. 5b shows the measured reflection coefficient below the −10 dB threshold.

Next, Fig. 6 shows the measurements for the 2×2 antenna. The conclusions that can be drawn from these experimental results are similar to those for the series-fed antenna. Measured radiation patterns measured in the main cuts, XZ and YZ planes, are presented in Figs. 7 and 8. Note that thick solid lines correspond to co-polar component while dashed lines to crosspolar ones. The directivity, beamwidth and stability of the patterns at the sampled frequencies validate the performance of both antennas. Specifically, at the center frequency, a directivity of 16 dBi and half-power beamwidth (HPBW) of 7° in YZ-plane for the 1-D array and 12 dBi and 32° HPBW for the 2-D antenna have been measured.

TABLE III: Measured gain in dBi of both antennas for both switching positions.

| Frequency (GHz) | 29.5 | 29.75 | 30.0 | 30.25 | 30.5 |
|---|---|---|---|---|---|
| 1×10 array (Pos.1) | 16.12 | 16.69 | 16.85 | 16.97 | 16.83 |
| 1×10 array (Pos.2) | 16.11 | 16.45 | 15.76 | 16.85 | 16.69 |
| 2×2 array (Pos.1) | 12.96 | 12.85 | 12.72 | 12.52 | 12.35 |
| 2×2 array (Pos.2) | 12.75 | 12.61 | 12.51 | 12.23 | 12.11 |

## IV. Conclusions

This paper presents two slotted array antennas operating in Ka-band with switchable circular polarization capability. The proposed mechanism allows easy switching between RHCP and LCHP and vice versa. Experimental results showed an axial ratio consistently below 3 dB from 29.5 GHz to 30.5 GHz for both switching positions in the two aluminum prototypes. Future lines of work should integrate the concept into a larger array as well as incorporate a motor to handle the mechanical switching.

## V. Acknowledgements

This work has been funded by the Spanish Goverment, Agencia Estatal de Investigacion (AEI), under project PID2019-107688RB-C22.

## References

[1] H. Fenech, A. Tomatis, S. Amos, V. Soumpholphakdy, and J. Serrano Merino, "Eutelsat hts systems," *International Journal of Satellite Communications and Networking*, vol. 34, no. 4, pp. 503–521, 2016.

[2] S. S. Gao, Q. Luo, and F. Zhu, *Introduction to circularly polarized antennas*. Wiley-IEEE Press, 2014.

[3] P. Naseri, S. A. Matos, J. R. Costa, C. A. Fernandes, and N. J. Fonseca, "Dual-band dual-linear-to-circular polarization converter in transmission mode application to $k/ka$-band satellite communications," *IEEE Transactions on Antennas and Propagation*, vol. 66, no. 12, pp. 7128–7137, 2018.

[4] M. Li, Y. Wu, W. Wang, and A. A. Kishk, "Wideband polarization reconfigurable differential circularly polarized antenna," *IEEE Access*, vol. 7, pp. 64 697–64 703, 2019.

[5] W. Lin, S.-L. Chen, R. W. Ziolkowski, and Y. J. Guo, "Reconfigurable, wideband, low-profile, circularly polarized antenna and array enabled by an artificial magnetic conductor ground," *IEEE Transactions on Antennas and Propagation*, vol. 66, no. 3, pp. 1564–1569, 2018.

[6] L. Ge, X. Yang, D. Zhang, M. Li, and H. Wong, "Polarization-reconfigurable magnetoelectric dipole antenna for 5g wi-fi," *IEEE Antennas and Wireless Propagation Letters*, vol. 16, pp. 1504–1507, 2017.

[7] D.-G. Seo, J.-H. Kim, M. M. Tentzeris, and W.-S. Lee, "A quadruple-polarization reconfigurable feeding network for uav rf sensing antenna," *IEEE Microwave and Wireless Components Letters*, vol. 29, no. 3, pp. 183–185, 2019.

[8] Y.-Y. Jeong and W.-S. Lee, "Wideband printed half bow-tie antenna array based on a quad-mode reconfigurable feeding network for uav communications," *IEEE Open Journal of Antennas and Propagation*, vol. 2, pp. 238–248, 2021.

[9] W. Lin and H. Wong, "Wideband circular-polarization reconfigurable antenna with l-shaped feeding probes," *IEEE Antennas and Wireless Propagation Letters*, vol. 16, pp. 2114–2117, 2017.

[10] X. Zhao, C. Yuan, L. Liu, S. Peng, Q. Zhang, and H. Zhou, "All-metal transmit-array for circular polarization design using rotated cross-slot elements for high-power microwave applications," *IEEE Transactions on Antennas and Propagation*, vol. 65, no. 6, pp. 3253–3256, 2017.

[11] M. Ferrando-Rocher, J. I. Herranz-Herruzo, A. Valero-Nogueira, and A. Vila-Jiménez, "Single-layer circularly-polarized $ka$-band antenna using gap waveguide technology," *IEEE Transactions on Antennas and Propagation*, vol. 66, no. 8, pp. 3837–3845, 2018.

[12] J. I. Herranz-Herruzo, M. Ferrando-Rocher, A. Valero-Nogueira, and B. Bernardo-Clemente, "Novel asymmetric t-shaped radiating element for circularly-polarized waveguide slot arrays," *IEEE Transactions on Antennas and Propagation*, pp. 1–1, 2021.

[13] J. I. Herranz-Herruzo, A. Valero-Nogueira, M. Ferrando-Rocher, B. Bernardo-Clemente, R. Lenormand, A. Hirsch, J.-L. Almeida, M. Arnaud, and L. Barthe, "Low cost switchable rhcp/lhcp antenna for sotm applications in ka-band," in *2015 9th European Conference on Antennas and Propagation (EuCAP)*. IEEE, 2015, pp. 1–4.

[14] K. Tekkouk, J. Hirokawa, R. Sauleau, and M. Ando, "Wideband and Large Coverage Continuous Beam Steering Antenna in the 60-GHz Band," *IEEE Transactions on Antennas and Propagation*, vol. 65, no. 9, pp. 4418–4426, 2017.

[15] A. Cherrette, R. D. Bruno, S. Brisbin, and G. Lok, "Hybrid electronic/mechanical scanning array antenna," Nov. 14 2017, uS Patent 9,819,082.

[16] M. Tripodi, F. DiMarca, T. Cadili, C. Mollura, F. DiMaggio, and M. Russo, "Ka band active phased array antenna system for satellite communication on the move terminal," in *Satellite Telecommunications (ESTEL), 2012 IEEE First AESS European Conference on*. IEEE, 2012, pp. 1–4.

[17] M. Ferrando-Rocher, J. I. Herranz-Herruzo, D. Sánchez-Escuderos, and A. Valero-Nogueira, "Dual circularly-polarized slot-array antenna in ka-band fed by groove gap waveguide," in *2020 IEEE International Symposium on Antennas and Propagation and North American Radio Science Meeting*. IEEE, 2020, pp. 421–422.

[18] M. Ferrando-Rocher, A. Valero-Nogueira, J. I. Herranz-Herruzo, A. Berenguer, and B. Bernardo-Clemente, "Groove gap waveguides: A contactless solution for multilayer slotted-waveguide array antenna assembly," in *2016 10th European Conference on Antennas and Propagation (EuCAP)*. IEEE, 2016, pp. 1–4.

[19] E. Rajo-Iglesias, M. Ferrando-Rocher, and A. U. Zaman, "Gap waveguide technology for millimeter-wave antenna systems," *IEEE Communications Magazine*, vol. 56, no. 7, pp. 14–20, 2018.

[20] M. Baquero-Escudero, A. Valero-Nogueira, M. Ferrando-Rocher, B. Bernardo-Clemente, and V. E. Boria-Esbert, "Compact combline filter embedded in a bed of nails," *IEEE Transactions on Microwave Theory and Techniques*, vol. 67, no. 4, pp. 1461–1471, 2019.

[21] M. Ferrando-Rocher, A. Valero-Nogueira, J. I. Herranz-Herruzo, and J. Teniente, "60 ghz single-layer slot-array antenna fed by groove gap waveguide," *IEEE Antennas and Wireless Propagation Letters*, vol. 18, no. 5, pp. 846–850, 2019.